Polyhedron 31 (2012) 345–351

Contents lists available at SciVerse ScienceDirect

Polyhedron

journal homepage: www.elsevier.com/locate/poly

A second crystal form of [Ni(2,2′-bipyridine)$(H_2O)_3(NO_3)](NO_3)$ featuring a different molecular orientation

Apinpus Rujiwatra [a], Saranphong Yimklan [a], Timothy J. Prior [b,*]

[a] Department of Chemistry and Centre for Innovation in Chemistry, Faculty of Science, Chiang Mai University, Chiang Mai 50200, Thailand
[b] Department of Chemistry, University of Hull, Cottingham Road, Hull HU6 7RX, UK

A R T I C L E I N F O

Article history:
Received 30 August 2011
Accepted 25 September 2011
Available online 12 October 2011

Keywords:
Nickel
2,2′-Bipyridine
Coordination complex
Crystal structure
Polymorph

A B S T R A C T

The molecular structure of a second form of [Ni(2,2′-bipyridine)$(H_2O)_3(NO_3)](NO_3)$ is reported. The previous report is for a blue monoclinic polymorph. The second form is orthorhombic and crystallises as green blocks with unit cell parameters $a = 9.1201(12)$ Å, $b = 14.444(2)$ Å, $c = 21.805(4)$ Å, $V = 2872.4(8)$ Å^3, $Z = 8$. The complex was characterised by elemental analysis, infrared spectroscopy, UV–Vis spectroscopy, and thermogravimetry. The bipyridine acts as a bidentate ligand to Ni^{2+} and the octahedral coordination is completed by three water molecules and one monodentate nitrate ion. A second nitrate forms hydrogen bonds to the bound water molecules. The difference between the two forms in terms of the molecular geometry is described in relation to other similar compounds. The key difference between the two forms is the orientation of the two nitrate anions, and hence the hydrogen bonding present.

1. Introduction

2,2′-Bipyridine is one of the most widely employed ligands in the synthesis of metal complexes [1]. At present there are over 5500 structures reported that feature 2,2′-bipyridine bound to a transition metal [2]. The vast majority of these (>99.6%) feature 2,2′-bipyridine acting as a bidentate ligand. There are many further examples that contain derivatives of 2,2′-bipyridine [1] and other similar ligands [3]. Complexes containing 2,2′-bipyridine have been widely used in studies of electron transfer [4] and chemiluminescence [5], and as model systems for optical isomerism [6].

In contrast to purely organic systems, it is somewhat unusual to observe polymorphism in inorganic compounds, particularly where two or more polymorphs are stable at the same temperature. Often the difference in crystal packing is accompanied by a change in colour, as is the case for some compounds containing 2,2′-bipyridine. For example, Pt(2,2′-bipyridine)Cl_2 exists as two different crystal forms under ambient conditions depending on the solvent employed: a red form [7] that crystallises in space group *Cmcm* and a yellow form [8] that adopts space group *Pbca*.

2,2′-Bipyridine has been utilised as an auxiliary (non-framework) ligand in the synthesis of coordination polymers. For example it has been used with metal ions and the framework formers 1,3,5-benzenetricarboxylate [9], squarate [10], and succinate [11]. We sought to employ 1,4-benzenedicarboxylic acid in the presence of a cation and 2,2′-bipyridine to synthesise similar frameworks. Our aim was to control the initial pH and ratio of reactants to influence the product obtained from hydrothermal synthesis. Here we report the structure of a second crystal form of the compound [Ni(2,2′-bipyridine)$(H_2O)_3NO_3](NO_3)$ and demonstrate that the structure determined at low temperature persists above room temperature. The relationship with earlier structure of the same composition is described in detail.

2. Materials and methods

2.1. Microwave synthesis

Crystals of the title compound were grown from a solution of 0.5826 g nickel(II) nitrate hexahydrate ($Ni(NO_3)\cdot 6H_2O$, Carlo Erba 99%) with 0.1562 g 2,2′-bipyridine ($C_{10}H_8N_2$, Fluka >99%) and 0.1670 g terephthalic acid ($C_6H_4(COOH)_2$, BDH 97%) in 10.00 cm^3 deionized water (Ni:nitrate:2,2′-bipyridine:terephthalic:water molar ratio = 2:2:1:1:556). Reagents were loaded into a 23 cm^3 Teflon lined pressure vessel. The reaction was performed for 3 h, under an autogenous pressure generated at 630 W (96 °C) using a domestic microwave oven (Whirlpool XT – 25ES/S, 900 W, 2.45 GHz). The initial pH of the solution was 3, measured using universal pH strips (Merck, 1.09535.0001). It may be noted that the pH of the solution did not change after the reaction.

The crystals obtained were present as aggregates of mid-green plates, separated from supernatant by filtration, then washed with deionized water and dried in air. The sample appeared visibly

---

* Corresponding author. Tel.: +44 (0)1482466389; fax: +44 (0)1482466410.
E-mail address: t.prior@hull.ac.uk (T.J. Prior).

0277-5387/$ - see front matter © 2011 Elsevier Ltd. All rights reserved.
doi:10.1016/j.poly.2011.09.046

homogeneous under magnification. X-ray diffraction analysis of several crystals at room temperature confirmed this. Satisfactory chemical analysis data were obtained for **2**.

2.2. X-ray diffraction analysis

Routine X-ray diffraction data collection and structure solution procedures were adopted. A single crystal of dimensions $0.21 \times 0.11 \times 0.06\ mm^3$ was cut from a larger aggregate, coated in perfluoropolyether oil and mounted at the end of a glass fibre. Data were collected in series of ω-scans using a Stoe IPDS2 diffractometer operating with Mo radiation. The crystal temperature was maintained using an Oxford Instruments nitrogen gas cryostream. The structure was solved by direct methods [12]. Full matrix least squares refinement against F^2 implemented within SHELXL [12] was employed for structure refinement.

Hydrogen atoms attached to 2,2′-bipyridine were positioned and refined using a riding model. Those of water were located in difference Fourier maps and their positions refined subject to the restraint that all O–H bond lengths were the same with a standard deviation 0.03 Å. Sensible restraints were also applied to the geometry of the water molecules.

For the first data collection the crystal was held at 120 K and a full set of data collected. Subsequently, the crystal was glued to the fibre and further sets of data frames collected, sufficient to determine the unit cell. The unit cell was determined at a further nine temperatures. A set of twenty data frames were collected at 353 K and the data from these were used to refine the structure at this temperature.

Routine X-ray diffraction data collection and structure solution procedures were adopted for form **1** using a crystal of dimensions $0.48 \times 0.12 \times 0.11\ mm^3$.

2.3. Spectroscopic characterisation

IR spectra were collected from ground crystals of **2** as a KBr disc, using a Bruker Tensor 27 FT-IR spectrometer (4000–400 cm^{-1}, resolution 0.5 cm^{-1}).

UV–Vis reflectance spectra were collected from lightly ground crystals loaded in a $BaSO_4$ matrix using a Cary 5E UV-vis-NIR Spectrophotometer.

2.4. Thermogravimetry

Samples were placed into platinum pans, loaded into a Mettler-Toledo TGA/DSC1 Thermogravimetric Analyzer and heated under a flow of nitrogen from room temperature to 1000 °C at a ramp rate of 30 °C min^{-1}.

3. Results and discussion

3.1. Crystal structure analysis

A report of the structure of $[Ni(2,2'\text{-bipyridine})(H_2O)_3NO_3](NO_3)$ at room temperature has appeared previously [13]. This compound (hereafter **1**) crystallises in the centrosymmetric monoclinic space group *P*2₁/*c* and is isostructural with the manganese analogue [14]. Here we describe a second crystal form (**2**) for this compound obtained under microwave-assisted hydrothermal conditions that displays the same connectivity as **1**, but differs in the orientation of the groups present. A description of the structure of **1** and its relation to **2** appears later.

The structure of **2** was initially determined at 120 K. At this temperature $[Ni(2,2'\text{-bipyridine})(H_2O)_3NO_3](NO_3)$ was found to crystallise in the centrosymmetric space group *Pbca* (number 61) with $Z' = 1$. Each Ni^{2+} is approximately octahedral in coordination geometry, bound to a bidentate molecule of 2,2′-bipyridine, three molecules of water, and a monodentate nitrate. The lengths of the coordination bonds about nickel are in good agreement with others of similar complexes. The CCDC [2] has 133 structures containing nickel, bipyridine, and ligated water. For these, the mean Ni–O (water) and Ni–N bond lengths are 2.08(4) and 2.07(4) Å, respectively, while the mean N–Ni–N angle is 79.0(15)°. For form **2** at 120 K, the bond lengths are 2.054(4), 2.078(4) and 2.083(5) Å (Ni–O), and 2.050(5) and 2.081(5) Å (Ni–N), while the N–Ni–N angle is 79.4(2)°. For 63 structures with monodentate nitrate and at least two pyridyl donors, the mean Ni–O (nitrate) bond length is 2.10(7)Å and for **2** this bond length is 2.082(4). A further uncoordinated nitrate anion forms hydrogen bonds to the bound water. The distance between hydrogen atoms of water and unbound nitrate are: 1.91(3) Å (O1–H1B···O10) and 1.94(3) Å (O2–H2B···O9). An ORTEP representation of **2** is shown in Fig. 1. Basic crystal data are given in Table 1.

The bound nitrate forms a single hydrogen bond to water in an adjacent complex. Every hydrogen atom of the three water molecules is involved in hydrogen bonding to nitrate. A full list of these is given in Table 2. There is a tendency to short, linear, hydrogen bonds with few bifurcated interactions (Fig. 2b). The combination of hydrogen bonds between the complexes and unbound nitrate generates infinite puckered sheets of thickness 5.552 Å that extend in the *xy* plane. These sheets are two molecules thick and the $[Ni(2,2'\text{-bipyridine})(H_2O)_3NO_3]^+$ ions are arranged such that the aromatic rings of the bipyridine are approximately perpendicular to the layers and project above and below them. The sheets are stacked along *c* in ABAB fashion at a separation of *c*/2 (10.903(4) Å). This arrangement facilitates two types of intermolecular interactions. The hydrogen bonding within the layer is illustrated in Fig. 2. Interdigitation of the aromatic rings on adjacent layers leads to relatively close approach of the π-systems of neighbouring bipyridine ligands. The distance between these is of the order of 3.43 Å; for example $C7^i$ ($i = x - ½, y, 1 - z$) lies 3.376(6) Å above the ring formed from N1 and C1–C5. This close approach is suggestive of a π–π interaction. In addition the proximity of H3 to an adjacent bipyridine ($H3 \cdots C9^{ii}$ = 2.80 Å, *ii* = −*x*,

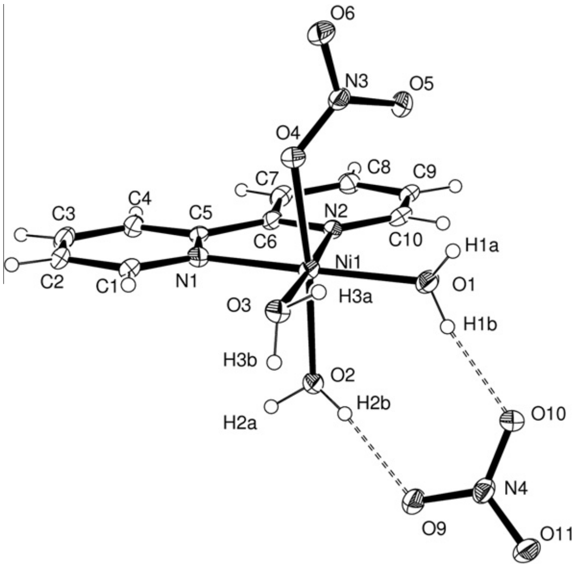

Fig. 1. ORTEP plot of the asymmetric unit of **2**. Atoms are shown as 30% thermal ellipsoids. Hydrogen bonds are illustrated by dashed lines. Selected bond lengths: Ni1–N1 2.081(5) Å, Ni1–N2 2.050(5) Å, Ni1–O1 2.054(4) Å, Ni1–O2 2.078(4) Å, Ni1–O3 2.083(5) Å, Ni1–O4 2.082(4) Å.

Table 1
Basic crystal structure and refinement data for form **1** and form **2**.

Identification code	[Ni(2,2′-bipyridine)$(H_2O)_3NO_3$](NO_3)	
	Form **1**	Form **2**
Empirical formula	$C_{10}H_{14}N_4NiO_9$	$C_{10}H_{14}N_4NiO_9$
Formula weight	392.96	392.96
Temperature (K)	120(2)	120(2)
Wavelength (Å)	0.71073	0.71073
Crystal system	Monoclinic	Orthorhombic
Space group	$P2_1/c$	*Pbca*
Unit cell dimensions	a = 11.2206(13) Å; b = 9.3513(7) Å; c = 14.8649(19) Å; α = 90° β = 109.793(9)° γ = 90°	a = 9.1201(12) Å b = 14.444(2) Å c = 21.805(4) Å
Volume	1467.6(3) $Å^3$	2872.4(8) $Å^3$
Z	4	8
Density (calculated) (mg m^{-3})	1.778	1.817
Absorption coefficient (mm^{-1})	1.380	1.411
F(000)	808	1616
Crystal size (mm)	0.48 × 0.12 × 0.11	0.21 × 0.11 × 0.06
Theta range for data collection (°)	2.62–27.51	2.80–26.00
Index ranges	$-14 \le h \le 14$, $-11 \le k \le 12$, $-19 \le l \le 19$	$-11 \le h \le 10$, $-15 \le k \le 17$, $-17 \le l \le 26$
Reflections collected	11 700	8454
Independent reflections	3371 [R_{int} = 0.0856]	2763 [R_{int} = 0.1057]
Completeness to theta = 26.00° (%)	99.9	98.1
Absorption correction	analytical	analytical
Maximum and minimum transmission	0.8701 and 0.6508	0.9201 and 0.7560
Refinement method	full-matrix least-squares on F^2	full-matrix least-squares on F^2
Data/restraints/parameters	3371/51/257	2763/19/237
Goodness-of-fit on F^2	0.951	0.906
Final *R* indices [$I > 2\sigma(I)$]	R_1 = 0.0358, $wR_{F^2} = 0.0825$	R_1 = 0.0581, $wR_{F^2} = 0.1237$
R indices (all data)	R_1 = 0.0526, $wR_{F^2} = 0.0871$	R_1 = 0.1115, $wR_{F^2} = 0.1383$
Largest difference peak and hole (e $Å^{-3}$)	0.950 and −0.795	0.698 and −1.237

½ + *y*, ½ − *z*) may suggest a C–H···π interaction. Therefore the structure is separated into two parts: hydrogen-bonded layers and regions where there is relatively close approach of the bipyridine aromatic rings; hydrophilic and hydrophobic parts, as shown in Fig. 3.

3.2. Further characterisation

The diffuse reflectance UV–Vis spectra for crystals of **1** and **2** are shown in Fig. 4. The low energy regions of the two spectra (5000–20 000 cm^{-1}) are remarkably similar. In each form the coordination about the Ni^{2+} ion is approximately octahedral, hence the broad absorptions centred around 10 000 and 16 000 cm^{-1} can be assigned to the transitions $^3A_{2g} \rightarrow {}^3T_{2g}$ and $^3A_{2g} \rightarrow {}^3T_{1g}$ (*F*), respectively [15]. The third band expected at around 27 000 cm^{-1} due to the transition $^3A_{2g} \rightarrow {}^3T_{1g}$ (*P*) is obscured by broad charger transfer absorption that extends into the visible region from the UV. The region of the spectrum due to charge transfer transitions to the 2,2′-bipyridine (above *ca.* 23 000 cm^{-1}) is rather different in the two compounds. This is in line with the observed colours of the two compounds; the green form (**2**) absorbs more light in the blue region of the spectrum than does form **1**. The inset within Fig. 4 highlights the difference in the features around 32 000 cm^{-1}.

The IR spectrum of **2** displays bands characteristic of the species present: bipyridine, nitrate, and water. The presence of hydrogen bonds between nitrate ions and water molecules is in good agreement with the broadening effect observed in the IR spectrum (supplied in the Supplementary data). In addition to the characteristic absorptions of the 2,2′-bipyridine ligands, an intense and broad absorption band in the range 3020–3670 cm^{-1} corresponds to coordinated water molecules [16]. A single absorption at 735 and doublet absorptions at 825 and 815 cm^{-1}, and at 1382 and 1414 cm^{-1} should correspond to the fundamental ν_4, ν_2 and ν_3 modes of the nitrate, respectively [17,18]. The lowered symmetry of nitrate in **2** results in the presence of ν_1 at 1025 and 1017 cm^{-1} in the IR spectrum, which otherwise be absent. Due to the presence of both monodentate and unbound nitrates, three absorption bands should be expected due to a combination of $[\nu_3 + \nu_4]$ in a region 1700–1800 cm^{-1}, two of which from the monodentate nitrate should separate by *ca.* 20–25 cm^{-1} [19]. The spectrum of **2** however shows only two absorptions (1790 and 1762 cm^{-1}) in this region, which is similar to earlier reports. The suppression of the third band on account of hydrogen bonding has been noted previously [13]. The difference in relative intensities of these two bands between **1** and **2** may be noted. While they are nearly equivalent in intensity in **1** [13], the absorption at 1790 cm^{-1} shows significantly lower intensity than that at 1762 cm^{-1} in the case of **2**.

Thermogravimetric data for **2** are contained the Supplementary data. The compound loses mass in two relatively well-defined steps. An initial weight loss in the region 30–200 °C corresponds to loss of the ligated water and some decomposition of nitrate to give a composition Ni(2,2′-bipyridine)$O_{0.33}(NO_3)_{1.67}$. At approximately 360 °C the phenanthroline ligands are lost to generate a composition with approximate RMM 118, which we tentatively assign as $NiO_{0.5}(NO_2)$. This further decomposes to give a mixture of NiO and Ni above 600 °C.

It was surprising that a different structure for this compound had been reported previously at room temperature and therefore we explored the crystal chemistry of **2** as a function of temperature. It was proposed that **2** might be a low temperature form of this compound that would change to **1** upon heating. The crystallographic unit cell was measured as a function of temperature up to 353 K. At this temperature the structure was determined again. The unit cell volume expanded smoothly as a function of temperature and there was no evidence for a change in the crystal symmetry. Although the crystal began to decay upon heating above 323 K, it was possible to refine the crystal structure using

Table 2
Hydrogen bonds within form **2**.

Hydrogen bond donor (D–H)	D–H bond length (Å)	H. . .Acceptor distance (Å)	D–H. . .A angle (°)	D...A distance (Å)	Acceptor atom (A) [symmetry operatory]
O1–H1A	0.84(3)	1.92(3)	173(7)	2.754(7)	O11 [$x - ½, -y + ½, -z$]
O1–H1B	0.83(3)	1.91(3)	170(7)	2.726(5)	O10
O2–H2A	0.85(3)	1.94(3)	169(7)	2.781(6)	O5 [$-x + ½, y + ½, z$]
O2–H2B	0.83(2)	1.94(3)	168(7)	2.761(6)	O9
O3–H3A	0.84(3)	2.23(3)	155(5)	3.015(6)	O10 [$x - ½, -y + ½, -z$]
O3–H3B	0.83(3)	2.00(3)	167(7)	2.816(7)	O9 [$-x + 1, -y + 1, -z$]

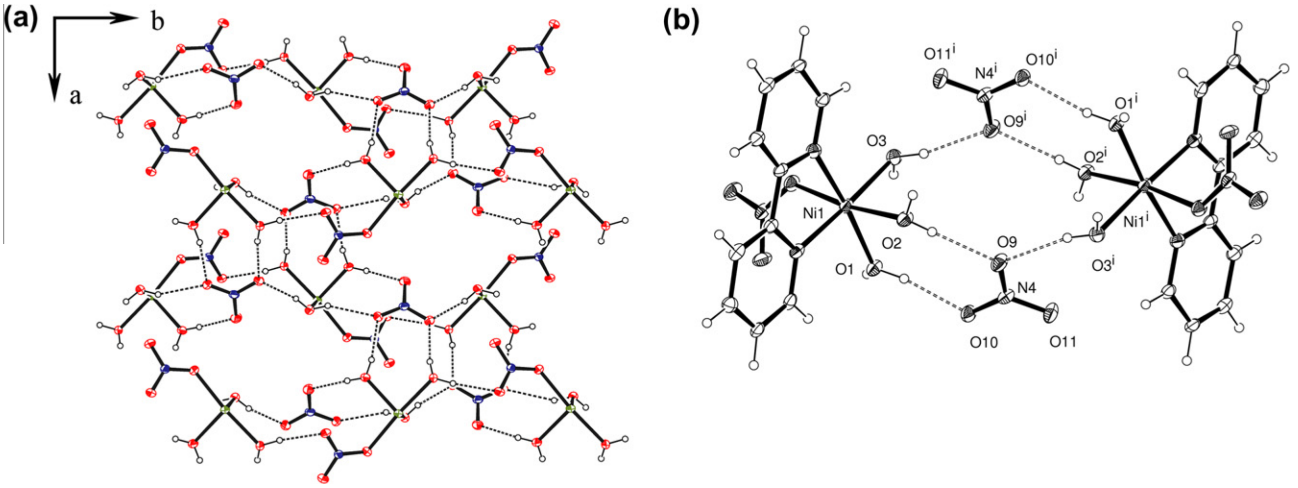

Fig. 2. (a) View of a single hydrogen-bonding layer in **2**. Bipyridine molecules have been omitted for clarity. (b) Two [Ni(2,2′-bipyridine)$(H_2O)_3NO_3$](NO_3) units forming a centrosymmetric embrace within the hydrogen bonding layer. Symmetry equivalent atoms are generated by the operator $i = 1 - x, 1 - y, -z$.

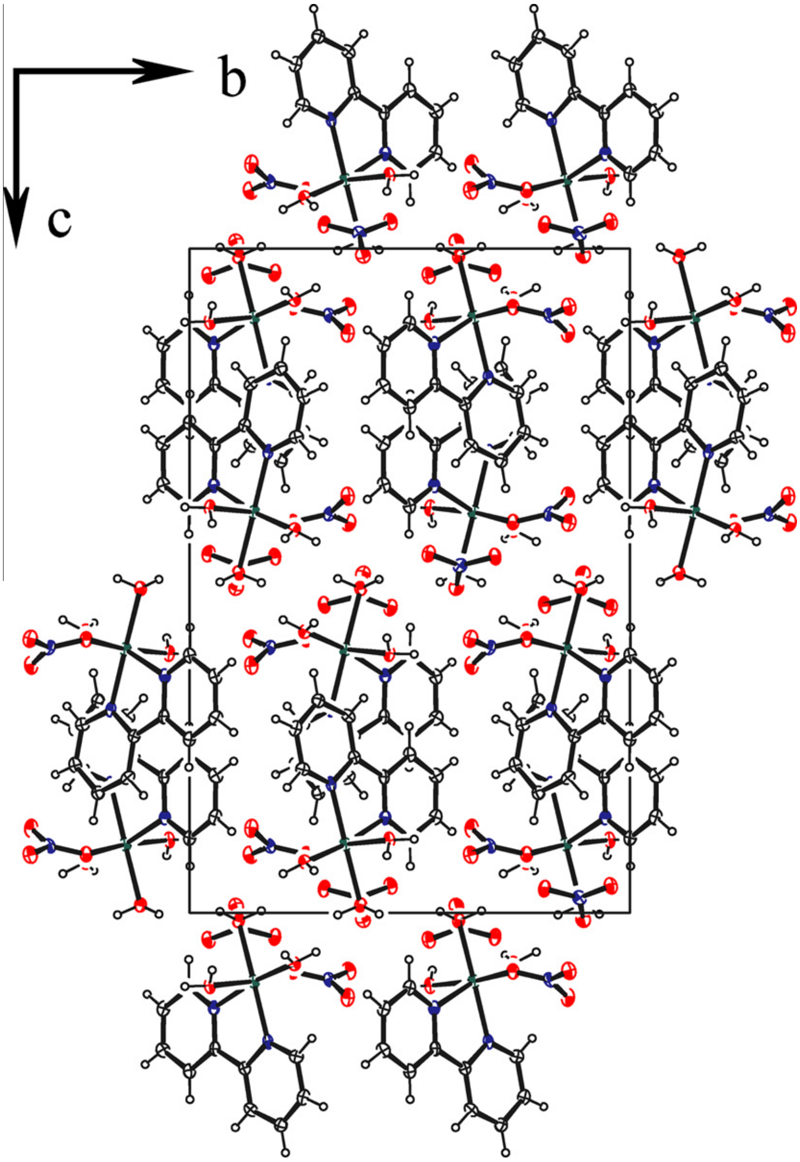

Fig. 3. View down *a* of the crystal packing in **2** to illustrate the arrangement of hydrogen-bonding layers.

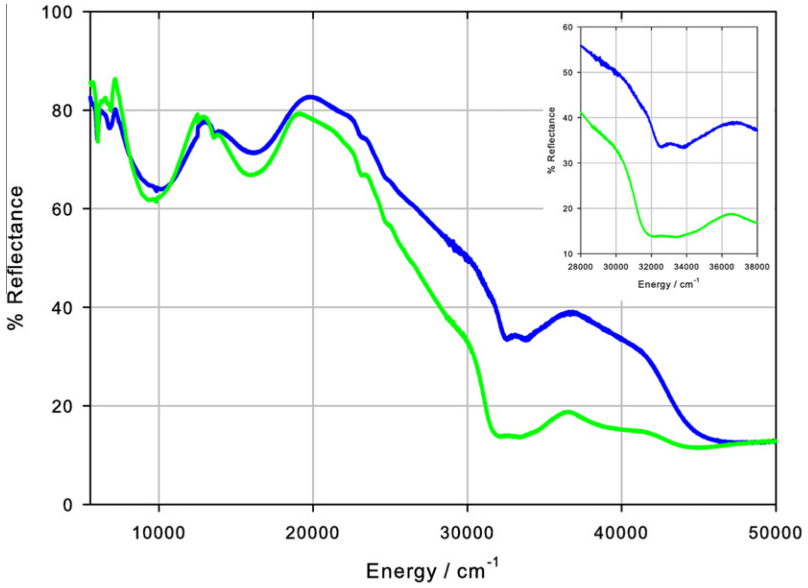

Fig. 4. UV–Vis spectra for form **1** (blue) and form **2** (green). Data for form **1** are shown in black and for form **2** in grey. The inset shows an expanded region of the spectrum between 28000 and 38000 cm^{-1}. (For interpretation of the references to color in this figure legend, the reader is referred to the web version of this article.)

data collected at 353 K. The principal structural features are preserved at this temperature. This suggests that it is not possible to convert between **1** and **2** by changing the temperature of the crystal. Full results of the variable temperature diffraction experiments are contained in the Supplementary information.

*3.3. Recrystallisation and crystal structure of form **1***

In the original report of form **1** [13] crystals were obtained from aqueous solution. Recrystallisation of form **2** from water returned green crystals of the same form, as demonstrated by X-ray diffraction. These crystals were dissolved in hot propan-2-ol to yield a pale blue solution which was allowed evaporate over a period of days and yielded light blue block-shape crystals, shown to be form **1** by X-ray diffraction. The structure of form **1** was redetermined at 120 K and found to be in good agreement with that published previously. Basic crystal data for form **1** are contained in Table 1 and full details of the crystal structure are given in the Supplementary information.

*3.4. Comparison between **1** and **2***

Compound **2** crystallises in the space group *Pbca* and although **1** crystallises in the space group $P2_1/c$, a direct subgroup of *Pbca*, there is no crystallographic relationship between the two cells. There are two obvious physical differences between these materials. Compound **1** is reported to crystallise from aqueous solution as blue plate-like crystals, while **2** is obtained from microwave-assisted hydrothermal synthesis as aggregates of green plates. The density of the two forms is somewhat different: at 120 K the calculated density of **1** is 1.778 g cm^{-3} but for **2** the density is calculated to be 1.817 g cm^{-3}.

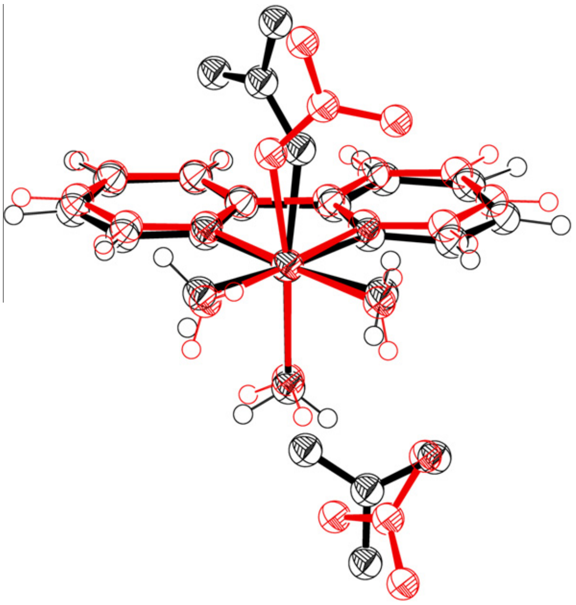

Fig. 5. Overlay of the asymmetric units of **1** and **2** viewed from approximately the same orientation. Compound **1** is shown in black.

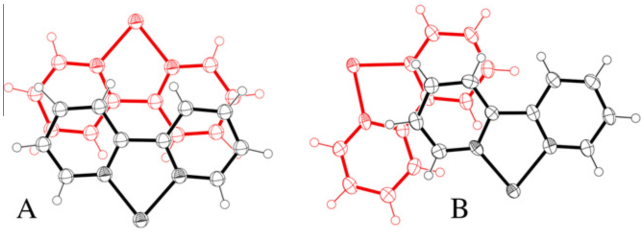

Fig. 6. Arrangement of adjacent π systems in **1** (A) and **2** (B).

The connectivity in the two forms is the same, as shown in Fig. 5, but the hydrogen bonding and relative arrangement of the nitrate ligands is different. The *rms* deviation of equivalent bonds between the two structures is 0.0217 Å (120 K), but there are slightly more pronounced differences for bound and unbound nitrate. For **1** Ni–N bond lengths are 2.0477(18) and 2.054(2) Å, but for **2**, these are 2.050(5) and 2.081(5) Å. The Ni–O bond lengths are similar: for **1** these are 2.0395(17), 2.0719(18), 2.0524(19), and 2.1014(17) Å, but for **2** they are 2.083(5), 2.054(4), 2.078(4) and 2.082(4) Å. For the six equivalent nitrate bonds the *rms* deviation is 0.0258 Å, although the means of N–O for bound and

Table 3
Comparison of the orientation of bound nitrate in **1** and **2** and the structures AFAYEL and NABPCU.

	Form **2**	Form **2**	Form **1**	Form **1** (KEBFAY)	AFAYEL	NABPCU
Metal	Ni	Ni	Ni	Ni	Mn	Cu
Temperature (K)	120	353	120	294	293	293
N–M–N (°)	79.4(2)	79.1(6)	79.71(8)	79.5(1)	72.8	81.6
M–O(nitrate) (Å)	2.082(4)	2.08(2)	2.1014(17)	2.103(1)	2.23	2.64
θ (°)	229.7(5)	227.9(13)	11.5(2)	8.0	14.81	9.46
φ (°)	127.8(3)	126.5(17)	131.03(14)	131.6	126.8	131.8
ω (°)	2.2(8)	7(2)	2.3(3)	−8.8	−10.2	−26.1

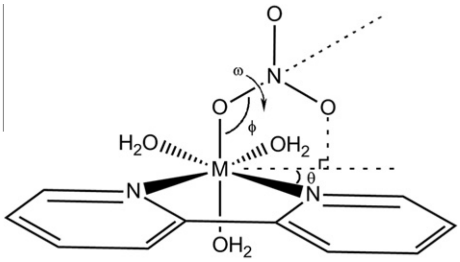

Fig. 7. Principle structural unit in **1** and **2** and other similar structures.

unbound nitrate in the two structures are the same within error. N–O bonds lengths in the bound nitrate are 1.260(3), 1.222(3), 1.273(3) Å for **1**, but 1.244(6), 1.253(6), 1.245(6) Å for **2**; N–O bond lengths in the unbound nitrate are: 1.230(3), 1.288(3), 1.235(3) Å for **1**, but 1.248(7), 1.255(6), 1.259(7) Å for **2**.

Differences in the positions of the bound and unbound nitrate are obvious from Fig. 5. There is hydrogen bonding present between water and nitrate and this assembles the complexes into layers which are two molecules thick and extend in the *yz* plane. The arrangement is similar to that in **2** but dominated by longer bifurcated hydrogen bonds to the unbound nitrate. Projecting from the layer and approximately perpendicular to it are the bipyridine ligands. The distance between bipyridine molecules from adjacent layers is 3.4869(14) Å which is suggestive of π–π interactions. The overlap of adjacent bipyridine molecules is more pronounced than in **2** as shown in Fig. 6, in line with other similar structures [20]. This suggests this is a more important stabilising factor in **1** than in **2**.

Aside from **2**, there are three other unique structures in the CCDC [2] that have the composition $[M(2,2'\text{-bipyridine})(H_2O)_3NO_3](NO_3)$. These are KEBFAY (**1**) (M = Ni), AFAYEL (M = Mn), and the family based on NABPCU01 (M = Cu). The last two compounds have very similar structures to **1**. The orientation of the bound nitrate in each of these structures can be quantified in terms of three angles and a bond length. At 120 and 353 K the structures of **2** are similar. The other three structures are distinct from these, but form a similar group. Data for the nitrate orientation are given in Table 3 and Fig. 7.

The difference in the UV–Vis absorption spectra of **1** and **2** appears to be the result of a change in the charge transfer absorption between the two forms. There are two major differences in the structures which may influence behaviour of the π-system of the 2,2′-bipyridine in charge transfer. In form **1**, an oxygen atom of bound nitrate lies directly above the π-system at a distance approximately 2.91 Å, but in form **2**, there is no such close approach because the orientation of this nitrate is different. In addition to this, as described above, there is evidence for greater π–π interactions in form **1** than in **2** (Fig. 6). These differences in the environment of the π-system in the two forms appears to have a distinct influence in their absorption in the charge transfer region and hence the colour of the two complexes.

4. Conclusion

The molecular structures of the two forms of $[Ni(2,2'\text{-bipyridine})(H_2O)_3NO_3](NO_3)$ principally differ in the orientation of the bound nitrate. This in turn has a profound effect on the crystal packing and hydrogen bonding within the solid state. Although the interconversion between the two forms involves only bond rotations and not covalent bond breaking, it is not possible to convert form **2** to form **1** thermally. However, this can be accomplished by recrystallisation from propan-2-ol. As is the case for other coordination compounds [7,8], the crystallisation conditions, particularly the solvent employed, have a direct influence on the crystal form obtained.

Acknowledgements

This work is financially supported by the National Research University Project under Thailand's office of the Higher Education Commission and the Thailand Research Fund. The authors are very grateful to Mr. Ian Dobson for the collection of thermogravimetry data and to Dr. Nigel Young for collection of UV–Vis spectra and helpful discussions.

Appendix A. Supplementary data

CCDC 838752 and 837641 contain the supplementary crystallographic data for **1** and **2**, respectively. These data can be obtained free of charge via http://www.ccdc.cam.ac.uk/conts/retrieving.html, or from the Cambridge Crystallographic Data Centre, 12 Union Road, Cambridge CB2 1EZ, UK; fax: (+44) 1223-336-033; or e-mail: deposit@ccdc.cam.ac.uk.

The other supplementary data comprise thermogravimetry and IR data of form **2**, crystal structure data for **2** at 353 K and details of variable temperature X-ray diffraction measurements, and full details of the structure of **1** at 120 K. Mol files for **1** and **2** are included.

Supplementary data associated with this article can be found, in the online version, at doi:10.1016/j.poly.2011.09.046.

References

[1] C. Kaes, A. Katz, M.W. Hosseini, Chem. Rev. 100 (2000) 3553.
[2] F.H. Allen, Acta Crystallogr., Sect. B 58 (2002) 380. see <www.ccdc.cam.ac.uk>.
[3] C.J. Sumby, Coord. Chem. Rev. 255 (2011) 1937.
[4] V. Balzani, G. Bergamini, F. Marchioni, P. Ceroni, Coord. Chem. Rev. 250 (2006) 1254.
[5] J.L. Adcock, C.J. Barrow, N.W. Barnett, X.A. Conlan, C.F. Hogan, P.S. Francis, Drug Test. Anal. 3 (2011) 145.
[6] J. Fan, T. Ziegler, Chirality 23 (2011) 155.
[7] W.B. Connick, L.M. Henling, R.E. Marsh, H.B. Gray, Inorg. Chem. 35 (1996) 6261.
[8] A.J. Canty, B.W. Skelton, P.R. Traill, A.H. White, Austr. J. Chem. 45 (1992) 417.
[9] Y. Wang, R. Cao, D. Sun, W. Bi, X. Li, J. Mol. Struct. 657 (2003) 301.
[10] R. Soules, F. Dahan, J.P. Laurent, P. Castan, J. Chem. Soc., Dalton Trans. (1988) 587.
[11] Z.H. Zhou, J.M. Yang, H.L. Wan, Cryst. Growth Des. 5 (2005) 1825.
[12] G.M. Sheldrick, Acta Crystallogr., Sect. A 64 (2008) 112.
[13] F. Walmsley, A.A. Pinkerton, J.A. Walmsley, Polyhedron 8 (1989) 689.

[14] X. Zhang, D. Huang, W. Wang, C. Chen, Q. Liu, Acta Crystallogr., Sect. C 58 (2002) m268.

[15] D. Nicholls, Complexes and First-Row Transition Elements, MacMillan, London, 1974.

[16] K. Nakamoto, Infrared and Raman Spectra of Inorganic and Coordination Compounds, Part B: Applications in Coordination, Organometallic, and Bioinorganic Chemistry, sixth ed., John Wiley & Sons, Hoboken, NJ, USA, 2009.

[17] A. Théorêt, C. Sandorfy, Can. J. Chem. 42 (1964) 57.

[18] J.A. Baran, M.A. Drozd, H. Ratajczak, J. Mol. Struct. 976 (2010) 226.

[19] A.B.P. Lever, E. Mantovani, B.S. Ramaswamy, Can. J. Chem. 49 (1971) 1957.

[20] S.G. Ang, B.W. Sun, Cryst. Growth Des. 5 (2005) 383.